Food Bioscience 57 (2024) 103505

Contents lists available at ScienceDirect

Food Bioscience

journal homepage: www.elsevier.com/locate/fbio

Vitamin E-fortified emulsion-templated oleogels structured with xanthan gum and soybean lecithin and their application in pound cakes

Su Jung Hong [a], Gye Hwa Shin [b,**], Jun Tae Kim [a,c,*]

[a] Department of Food and Nutrition, Kyung Hee University, Seoul, 02447, Republic of Korea
[b] Department of Food and Nutrition, Kunsan National University, Gunsan, 54150, Republic of Korea
[c] BioNanocomposite Research Center, Kyung Hee University, Seoul, 02447, Republic of Korea

ARTICLE INFO

Keywords:
Emulsion-template
Vitamin E
Oleogels
Solid fat replacer

ABSTRACT

Vitamin E-fortified oleogels (E-OGs) were prepared by vitamin E-loaded emulsion template using xanthan gum (XG) and soybean lecithin (SL) as oleogelators. Optimum processing conditions of E-OGs were obtained with 0.3% XG and 2.0% SL, which exhibited a small particle diameter of 651.50 ± 23.84 nm and adequate zeta potential of −30.20 ± 2.95 mV. This zeta potential value indicates that E-OGs are very stable due to the electrostatic repulsion between particles. The oil binding capacity (OBC) of E-OGs maintained above 99.97% when the XG concentration was 0.30% or more, whereas the OBC containing 0.15% XG significantly decreased from 99.84% to 96.79% after 5 days of storage. The E-OGs prepared at 0.3% XG or higher exhibited solid-like behavior with higher G' than G" in the results of the frequency sweep test. Solid-like behavior of E-OGs has some advantage such as ease of process, handling, and storage stability. E-OGs have been applied in pound cake manufacturing to replace commercially available butter. The rheological properties of the pound cake were analyzed using a texture profile analyzer. The hardness of the pound cake decreased significantly from 9.73 ± 1.33 N to 7.95 ± 0.58 N, and the porosity increased as butter was replaced with E-OGs, showing the potential of E-OGs to improve the quality of bakery products. E-OGs may also provide the benefits of vitamin E fortification. These results highlight the promising prospects of E-OGs in the food industry, particularly in the development of healthier and functional foods.

1. Introduction

Solid fats, which are energy sources and storage in the human body, play important roles in the mouthfeel, texture, and flavor of the food product. However, it is well known that it negatively influences on human health by increasing the risk of coronary artery disease, diabetes, and obesity because of high levels of trans and saturated fatty acids (Demirkesen & Mert, 2020). In 2019, the World Health Organization (WHO) recommended that the amount of saturated fat and trans fat should be less than 10% of total energy intake and 1% of total energy intake, respectively. Moreover, WHO has launched a 'REPLACE' campaign to encourage the replacement of industrially produced trans fats with healthier fats and oils (Pușcaș, Mureșan, Socaciu, & Muste, 2020). Despite these health concerns, processed foods high in solid fats continue to dominate the market and practical solutions, such as research into oleogels as healthy alternatives are urgently needed.

The oleogelation technique has been used in the fabrication of a substitute for solid fats by structuring vegetable oil using an oleogelator (Chuesiang et al., 2022). Oleogel is a solid fat-like gel composed of liquid oil in which a continuous phase and a three-dimensional network are formed using an oleogelator. Oleogels can exhibit rheological properties similar to solid fats without altering the chemical and nutritional profiles of vegetable oils (Pușcaș et al., 2020). In general, oleogels have been prepared by indirect and direct approaches. A direct method was to add an oleogelator, such as wax, to the liquid oil by heating and mechanical force (Zhang, Chuesiang, Kim, & Shin, 2022). The direct method can lower the existing saturated fat content but has the disadvantage of still containing a certain amount of saturated fat. Therefore, there has been increased interest in indirect approaches utilizing biopolymers as oleogelators, including emulsion, aerogels, or foam-templating techniques to remove or replace water and form oleogels (Li, Xi, Wu, & Zhang, 2023).

Recently, various studies have been reported on oleogels using

* Corresponding author. Department of Food and Nutrition, Kyung Hee University, Seoul, 02447, Republic of Korea.
** Corresponding author.
E-mail addresses: winnie19@kunsan.ac.kr (G.H. Shin), jtkim92@khu.ac.kr (J.T. Kim).

https://doi.org/10.1016/j.fbio.2023.103505
Received 25 July 2023; Received in revised form 4 December 2023; Accepted 17 December 2023
Available online 22 December 2023

encapsulation system templates, such as emulsion and nanostructured lipid carriers. Wang et al. (2023) investigated the comparison of properties of oleogels prepared using emulsion and foam as templates. Interestingly, the emulsion-template oleogel showed solid-like properties with 100% oil retention capacity, while foam-template oleogel showed semi-solid-like properties. Other researchers have also reported the application of fabricated oleogels to food products (Zou et al., 2022).

Vitamin E has been considered an excellent bioactive compound that exhibits many health benefits such as antioxidant, anti-inflammatory, and anticancer properties (Manosso, Camargo, Dafre, & Rodrigues, 2022). Vitamin E deficiency is very common in underdeveloped countries and the most common cause is insufficient vitamin E intake. In the United States, 89.8% of men and 96.3% of women aged over 19 years were found to have insufficient vitamin E intake (Sapiejka et al., 2018). Vitamin E is essential for preventing cardiovascular diseases, including coronary heart disease and atherosclerosis (Violi, Nocella, Loffredo, Carnevale, & Pignatelli, 2022). These limitations make it difficult to get sufficient amounts of vitamin E through fortified foods. However, vitamin E is poorly absorbed in the intestine and its bioavailability after oral administration is very low because of its fat-soluble nature (Goh, Ching, Ng, Chuah, & Julaihi, 2022).

Delivery systems such as emulsions, liposomes, and nanostructured lipid carriers have been reported as ideal methods to improve the solubility, body absorption, and bioavailability of fat-soluble functional ingredients such as vitamin E (Hong, Garcia, Park, Shin, & Kim, 2019). In addition, a carefully designed delivery system that protects vitamin E from physical or chemical attack during processing and storage makes it possible to apply vitamin E to various food applications. An emulsion is a dispersed colloidal system in which there are two or more immiscible liquids consisting of a dispersed phase (discontinuous or internal phase) in another liquid (continuous or external phase) stabilized by emulsifiers or physical treatments (Jafarifar et al., 2022). The emulsion system has been most commonly used to encapsulate and deliver a variety of bioactive lipids because it exhibits a wide range of rheological properties from low-viscosity liquids such as milk to high-viscosity (viscoelastic) solids such as butter and margarine (Erramreddy, Tu, & Ghosh, 2017). Among the emulsifiers, SL is a common ionic emulsifier used in the food industry because there are no particular restrictions on the amount used (Balcaen, Steyls, Schoeppe, Nelis, & Van der Meeren, 2021; Wang et al., 2021). However, since lecithin alone cannot effectively stabilize emulsions, many studies have reported on the use of mixtures of lecithin and polysaccharides as a thickener or stabilizer (Balcaen et al., 2021; Clausse, Lanoisellé, Pezron, & Saleh, 2018). It is well known that xanthan gum (XG) is an anionic heteropolysaccharide that can increase the viscosity and stability of emulsions by forming a double helix structure (Xing et al., 2022).

To the best of our knowledge, there are no reports on the processing and application of edible oleogels incorporated with vitamin E so far. The primary objective of this study was to demonstrate that E-OGs can effectively replace solid fats in terms of rheological properties and oxidative stability. The prepared E-OGs were further characterized by measuring the release profile and lipid digestion under simulated *in vitro* gastrointestinal conditions. Characterization of oxidative stability and lipid digestion provides a comprehensive understanding of the performance of E-OGs and the potential as a healthy alternative to traditional solid fats. Additionally, the E-OGs were applied to prepare pound cakes instead of butter, with a specific focus on the rheological properties of pound cakes.

2. Materials and methods

2.1. Materials

Vitamin E was purchased from DSM Nutritional Products Ltd. (Heerlen, Netherlands). Soybean oil, XG (viscosity (1% solution in 1% KCl): 1200–1600 cPs), and soybean lecithin (SL, 100%) were obtained from Ottogi Corp., Ltd. (Anyang, South Korea), Deosen Biochemical (Ordos) Ltd. (Ordos, Inner Mongolia, China), and Solae LLC. (St. Louis, MO, USA), respectively. Rabbit gastric extract for gastric lipase was purchased from Lipolytech® (Marseille, France). Pepsin, pancreatin, lipase, and bile salt were purchased from Sigma-Aldrich (St. Louis, MO, USA).

2.2. Preparatin of oleogels (OGs) and vitamin E-fortified oleogels (E-OGs)

Vitamin E-fortified oleogels (E-OGs) were prepared using an emulsion template structured with XG and SL. First, XG was dissolved in distilled water overnight as an aqueous phase. The oil phase was prepared by dissolving vitamin E and SL in 12 g of soybean oil. The coarse emulsion was prepared by adding the aqueous phase to the oil phase in a weight ratio of 6:4 and was then subjected to a probe-type of ultrasonication (VCX-750, Sonics & Materials Inc., Sandy Hook, CT, USA) at 20 kHz and 40% amplitude for 5 min. Ultrasonication was used to make a uniform emulsion from the coarse emulsion and then the final emulsion was freeze-dried for 72 h to prepare E-OGs. For comparison, the control oleogels (OGs) were also prepared using the same procedure without vitamin E. The prepared E-OGs and OGs were added at 50 g per Falcon tubes, completely sealed with parafilm, and stored at −20 °C until characterized.

2.3. FTIR and TGA analysis

The infrared spectra of the samples were analyzed using a Fourier-transform infrared (FT-IR) spectrometer (JASCO Spectroscopy FT-IR 4X, JASCO Co., Tokyo, Japan). A background scan was initially recorded and subsequent FT-IR analyses of the samples was performed at room temperature (25 ± 2 °C). The spectral scanning range was 4000–500 cm^{-1} and the resulting peaks were subjected to detailed analysis. Thermal stability was assessed by thermogravimetric analysis (TGA) utilizing a TGA 55 (TA Instruments, New Castle, DE, USA). Approximately 10–12 mg of sample was placed in a platinum pan heated from room temperature to 600 °C at a rate of 10 °C/min under a nitrogen gas flow of 50 mL/min.

2.4. Oil binding capacity (OBC)

The centrifuge method was used to measure the OBC of OGs according to the method of Blake and Marangoni (2015) with slight modifications. Firstly, the produced OGs were conditioned at 25 °C and 50% relative humidity (RH) for 3 h, and the samples were centrifuged at 11,515×*g* at 4 °C for 15 min (Model-1248R, Gyrozen Co. Ltd., Seoul, Korea). Then centrifuge tubes were reversed onto a filter paper to remove the spilled oil over time. OBC of OGs was calculated using the following equation (1):

$$\mathrm{OBC}\ (\%) = \left(1 - \frac{m_2}{m_1}\right) \times 100 \quad (1)$$

where m_1 is the mass of the sample before centrifugation and m_2 is the mass after removing the spilled oil.

2.5. Rheological properties

The dynamic viscoelastic properties of OGs were measured using a HAAKE rotational rheometer (RheoStress 1, Thermo Fisher Scientific, Karlsruhe, Germany) equipped with a 35 mm parallel plate geometry. The samples were subjected to dynamic oscillation in the frequency range of 0.01–100 Hz. Storage modulus (G′) and loss modulus (G″) of OGs as a function of angular frequency (0.1–100 rad/s) were measured at 20 °C.

2.6. Oxidative stability

The Schaal oven test was used to analyze the accelerated oxidation stability of butter, and soybean oil, and produced OGs according to the method of Li, Wan, Cheng, Liu, and Han (2019) with slight modifications. This is used as an accelerated oxidation assessment and exposes the sample to high temperatures for a short period. This test is designed to assess product shelf life and stability by estimating the behavior of samples over long periods under ambient conditions or typical storage conditions. Samples were stored in the lightproof oven at 60 °C for 12 days; peroxide value (PV) and ρ-anisidine value (ρ-AV) were measured every 2 days according to AOCS official method (CD 8b-90) and AOCS official method (CD 18–90), respectively. PV is the reactive oxygen contents indicating primary oxidation including oxidative rancidity where ρ-AV indicates secondary oxidation products which are responsible for off-flavors and odors. The total oxidation (TOTOX) value of OGs was calculated by the following equation (2):

$$\mathrm{TOTOX} = 2\mathrm{PV} + \rho\text{-}AV \tag{2}$$

where the *PV* is the peroxide value, and ρ-*AV* is the ρ-anisidine value.

2.7. In vitro digestion of E-OGs

Simulating the oral, gastric, and small intestine stages in digestive analysis is important for understanding how food components are broken down and absorbed in the human body. *In vitro* digestion studies allow us to investigate the effects of foods and formulations on nutrient release and absorption. In particular, faithful replication of the gastric and small intestine stages is crucial for studying the digestion of dietary fats, in which gastric lipase and pancreatic lipase play important roles. Monitoring the release of free fatty acids during intestinal digestion can provide insight into lipid hydrolysis efficiency and absorption. The digestion process which consisted of the oral, gastric, and small intestine phases was simulated using the standardized INFOGEST protocol (Brodkorb et al., 2019) with slight modifications. The enzyme activity of pepsin (2000 U/mg), gastric lipase (60 U/mg), pancreatic lipase (2000 U/mg), and pancreatin (100 U/mg) in total digesta was adjusted just before the start of each digestion procedure according to the protocol (Minekus et al., 2014). Supplementary Table S1 shows the compositions of simulated saliva fluid (SSF), simulated gastric fluid (SGF), and simulated intestinal fluid (SIF).

In the oral phase, 0.5 g of E-OGs was mixed with 9.5 g of SSF and then the pH was adjusted to 7 with 0.1 N (normality) NaOH. The mixture was incubated under shaking at 37 °C for 2 min.

In the gastric phase, 10 g of oral bolus and 10 g of SGF were mixed, 2000 U of pepsin and 60 U of gastric lipase were added, the pH was adjusted to 2 with 0.1N HCl, and stored at 37 °C for 2 h.

In the intestinal phase, 20 g of gastric chyme passed through the gastric phase, and 20 g of SIF were mixed, and 100 U of pancreatin, 2000 U of pancreatic lipase, and 10 mM of bile salt were added.

Free fatty acids (FFAs) released from the E-OGs during intestinal digestion (at 37 °C for 2 h) were titrated with a pH-stat (907 Titrando, Metrohm, Herisau, Switzerland). The amount of 0.1 N NaOH used during the pH adjustment to 7 is used to calculate the amounts of FFAs released as following equation (3):

$$\text{FFAs released } (\%) = \frac{V_{NaOH} \times M_{NaOH} \times M_{Lipid}}{W_{Lipid} \times 2} \times 100 \tag{3}$$

where V_{NaOH} is the volume of NaOH (L), M_{NaOH} is the concentration of NaOH (0.1 N), M_{Lipid} is the molecular weight of lipid (g/mol), and W_{Lipid} is the total mass of lipids in the intestinal phase (g).

2.8. Confocal Laser Scanning Microscopy (CLSM)

Morphological changes in E-OGs were observed during *in vitro* digestion using a Confocal Laser Scanning Microscope (C LSM 710, Zeiss, Gottingen, Germany). To facilitate this analysis, soybean oil and XG were first stained with Nile Red (0.02% w/v) and Calcofluor White (3%), respectively. Nile Red was used to monitor changes in the lipid phase (soybean oil), and Calcofluor White visualized the morphological changes of XG during the digestion of E-OGs. The excitation wavelengths were 515–530 nm for Nile Red and 440 nm for Calcofluor White.

2.9. Preparation of pound cakes

To evaluate the applicability of E-OGs as a solid fat replacer, pound cakes in which solid fat was replaced with E-OGs at various levels (0, 20, 40, 60, 80, and 100% by weight) were prepared. Firstly, 300 g fats (E-OGs, butter, or soybean oil) and 300 g sugar were blended for 3 min using a Horbart N50 mixer (Hobart, North York, Ontario, Canada) at speed 2, and 300 g whole egg was added and mixed at speed 2 for 5 min. Then, 300 g wheat flour, 32 g non-fat dry milk, 13 g baking powder, and 2 g salt were added to the above mixture at speed 2 for 2 min. Water (200 g) was added and mixed at speed 2 for 2 min. It was then scraped off to form batters. The batters (90 g) were poured into pans and baked in the oven (upper temperature 185 °C, bottom temperature 180 °C) for 30 min.

2.10. Texture profile analysis (TPA)

The texture profile of the prepared pound cakes was analyzed using a Universal Testing Machine (UTM; Z010TN, Zwick GmbH & Co. KG, Ulm, Germany). A pound cake sample (2 × 2 × 2 cm) was taken from the center of the cake and placed on a flat plate, and a probe of 3.5 cm diameter was compressed to 50% of the initial height at a speed of 10 mm/min. All measurements were performed at room temperature and at least 5 times.

2.11. X-ray micro-computed tomography (CT) analysis

The cross-sectional images of the prepared pound cakes were non-destructively visualized by a high-resolution desktop X-ray micro-CT system (XT H 225, Nikon Corp., Tokyo, Japan). Samples (4 cm horizontal x 4 cm vertical x 3 cm height) were taken from the center of the cake and placed parallel to the top and bottom surfaces. This sample was mounted on a rotary stage inside the Micro-CT instrument and scanned at a voltage of 100 kV, a current of 180 μA, and an exposure time of 250 ms. The images were stacked using a myVGL 3.0 software (Volume Graphics GmbH, Heidelberg, Germany) to generate 3D images in which the pore space is displayed as a black area. The total porosity (%) was also obtained from the images.

2.12. Statistical analysis

All measurements were performed in triplicate using freshly prepared samples and were reported as calculated means and standard deviations (mean ± SD). Statistics on a completely randomized design were performed by one-way analysis of variance (ANOVA) using SPSS software (SPSS Inc., Chicago, IL, USA). Duncan's multiple range test ($p < 0.05$) was used to detect differences among the means.

3. Results and discussion

3.1. Characterization of emulsion with different XG and SL concentrations

Table 1(a) shows the effect of XG concentrations (0.15, 0.3, 0.45, 0.6, and 0.75%) on the particle size and zeta potential of the emulsion containing 2.0% SL. As the increasing XG concentration of the aqueous phase formed the outer layer of the particles, the particle size significantly ($p < 0.05$) increased from 521.67 ± 12.43 nm to 1372.17 ±

Table 1
Particle size and zeta potential of emulsions with different XG (a) and SL (b) concentrations.

(a)		
XG concentration	Particle size (nm)	Zeta potential (mV)
XG-0.15/SL-2.0	521.67 ± 12.43[a,*]	−23.26 ± 1.72[d]
XG-0.30/SL-2.0	651.50 ± 23.84[b]	−30.20 ± 2.95[c]
XG-0.45/SL-2.0	739.47 ± 6.79[c]	−34.08 ± 3.92[c]
XG-0.60/SL-2.0	977.70 ± 36.46[d]	−43.76 ± 5.60[b]
XG-0.75/SL-2.0	1372.17 ± 21.36[e]	−51.05 ± 3.28[a]
(b)[b]		
SL concentration	**Particle size (nm)**	**Zeta potential (mV)**
XG-0.30/SL-0.4	3025.23 ± 305.53[c]	−21.50 ± 1.69[b]
XG-0.30/SL-1.2	1272.17 ± 21.36[b]	−27.19 ± 0.21[b]
XG-0.30/SL-2.0	651.50 ± 23.84[a]	−30.20 ± 2.95[b]
XG-0.30/SL-2.8	605.50 ± 12.64[a]	−44.85 ± 6.43[a]
XG-0.30/SL-3.6	521.67 ± 12.43[a]	−52.70 ± 9.72[a]

[*] Different letters on the same column indicate a significant difference at $p < 0.05$ ($n = 3$).

[b] In Table 1, please distinguish the SL concentration, particle size, and zeta potential in (b) with a bold line as in (a) above.

21.36 nm. The increase in particle size at higher XG concentrations can be attributed to their ability to produce a thick and gel-like matrix when mixed with liquid. XG molecules entangle and retain water, causing the particles to expand. As XG concentration increases, a more extensive molecular network is formed, resulting in larger particle sizes due to the water trapping and thickening properties of XG. This behavior is commonly observed when XG is used as a thickening or gelling agent (Huang, Kakuda, & Cui, 2001; Zhao, Zhao, Yang, & Cui, 2009). On the other hand, the zeta potential was significantly ($p < 0.05$) decreased from −23.26 ± 1.72 mV to −51.05 ± 3.28 mV as the XG concentration increased. The decrease in zeta potential with increasing XG concentration can be attributed to the electrostatic interaction and stabilizing influence of XG in the emulsion system (Cai et al., 2018). XG contains negatively charged functional groups such as carboxyl groups, which contribute to the generation of a negative zeta potential (Mirhosseini, Tan, Hamid, & Yusof, 2008). Generally, it is usually considered a stable emulsion when the absolute value of the zeta potential of an emulsion is more than 30 mV (Hong, Garcia, Shin, & Kim, 2022). Therefore, it was found that selecting 0.3% XG concentration was the optimal choice. This concentration achieved the highest oil content while maintaining a small particle size (651.50 ± 223.84 nm) and stable zeta potential (−30.20 ± 2.95 mV). This dual advantage of ensuring adequate stability (as expressed by zeta potential) and achieving the most consistent particle size is achieved while minimizing the use of polymers and SL, making it well-suited for commercial applications.

Table 1(b) shows the effect of SL concentrations (0.4, 1.2, 2.0, 2.8, and 3.6%) on the particle size and zeta potential of the emulsion containing 0.3% XG. As increasing SL concentration as an emulsifier, the particle size of the emulsion significantly ($p < 0.05$) decreased from 3196.4 ± 477.03 nm to 528.27 ± 8.70 nm. Park, Garcia, Shin, and Kim (2018) reported a similar phenomenon in that the particle size of the encapsulation system was formed uniformly and decreased with the emulsifier concentration. The zeta potential was significantly ($p < 0.05$) decreased from −22.11 ± 4.22 mV to −50.85 ± 1.79 mV as SL concentration increased. The increasing negative charge of the emulsion can be explained by the presence of anionic phospholipids in SL as well as by the adsorption of OH^- species to the oil-water interface. It shows a stable zeta potential value (−29.32 ± 1.43 mV) that does not induce particle aggregation over 1.2% SL concentration. Therefore, the emulsion prepared by selecting the formulation of 0.3% XG and 1.2% SL was lyophilized to prepare an emulsion-templated OGs.

3.2. Characterization of OGs

The physical properties of emulsion-templated OGs were compared with different XG concentrations. Fig. 1a exhibits OBC values representing the ability to retain the soybean oil of a three-dimensional network of the OGs. The OGs prepared at 0.3% or higher XG concentration showed over 99.99% OBC by 120 h storage, while the OBC of OGs prepared at 0.15% XG was significantly ($p < 0.05$) decreased from 99.84% ± 0.04%–96.79% ± 0.08% after 120 h storage. The removal of water from well-formed emulsion via freeze drying retains oil droplets closely and firmly packed (Patel et al., 2015). At 0.15% XG concentration, the XG interface of the oil droplet was not sufficient to hold the oil inside, and the surrounding wall of the oil droplet was broken and coalesced, further reducing the OBC after centrifugation (Pan et al., 2021). The decline in OBC suggests that OGs may have difficulty keeping soybean oil reserves stable within their structures over time. This can cause oil separation or migration, which can make the OGs unstable. This instability can manifest itself as changes in texture, appearance, and overall product quality, which are generally undesirable characteristics in a variety of food and product applications.

Storage modulus (G′) and loss modulus (G″) of the OGs with different XG concentrations were investigated by frequency sweeps (Fig. 1b). The G′ and G″ represent the elastic and viscous characteristics of the sample, respectively (Oh, Lee, Lee, & Lee, 2019). As XG concentration increased, the G′ and G″ of OGs increased, indicating that a gel with high elasticity and viscosity was formed. The increase in both G′ and G″ at higher XG concentrations is due to the ability of XG to form more substantial and structured networks within OGs. As the XG concentration increases, more XG molecules are available to interact and create a dense molecular matrix within the OGs (Alloncle & Doublier, 1991). This matrix contributes to the overall G′ and G″ of OGs, resulting in a gel-like structure with improved mechanical properties, and a similar trend has been reported in rice starch and XG mixture (Kim & Yoo, 2006). The OGs prepared above the 0.3% XG concentration exhibited a higher G′ value than G″ value, while the OGs prepared with 0.15% XG concentration exhibited a higher G″ value than G′ value. It is well known that

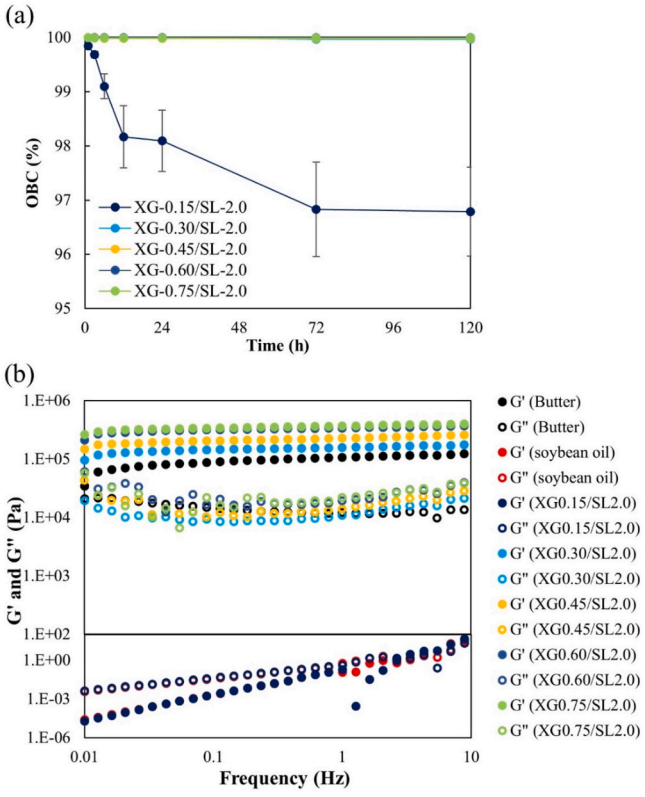

Fig. 1. Oil binding capacity (a) and rheological properties (b) of emulsion-templated oleogels with different xanthan gum concentrations.

the smaller G″ value than the G′ value of the samples exhibits solid-like behavior (Meng, Guo, Wang, & Liu, 2019). These properties are important in a variety of food processing fields, where products must maintain their structural integrity and shape, as seen in commercially available butter. OGs with higher G′ values are therefore more likely to mimic the properties of commercially available butter and perform effectively in applications requiring solid-like behavior.

FT-IR analysis was used to perform structural characterization for XG, SL, OGs, and E-OGs, and the results can be seen in Fig. 2a. The XG spectrum showed absorption peaks in the range of 3000–3500 cm^{-1}, which could be attributed to the O–H axial deformation. The band at 1710 cm^{-1} represents the C═O stretching vibration, and the band around 1600 cm^{-1} represents the axial deformation of the C–O portion of the enols (Said et al., 2021). Additionally, strong absorption bands between 1200 and 1000 cm^{-1} are associated with the stretching vibrational mode of C–O–H group and C–O–C of glycosidic moiety originating from the pyranose rings (Vázquez et al., 2020). For SL, a peak is observed at approximately 3300 cm^{-1}, which corresponds to O–H stretching. The strong absorption bands ranging from 2900 to 2800 cm^{-1} are attributed to the asymmetric and symmetric stretching vibrations of CH_2 and CH_3 groups, while the additional peak at 1700 cm^{-1} represents the C═O stretching frequency (Michał, Ewa, & Tomasz, 2015). Additional stretching vibrational peaks at 1170 cm^{-1} and 1050 cm^{-1} are the result of intramolecular C–O and C–C bonds (Siyal et al., 2020). Both OGs and E-OGs exhibited peak characteristics of XG and SL, confirming successful structuring by oleogelator. The additional peak observed at 1080 cm^{-1} in E-OGs is attributed to the plane bending of the phenyl group of vitamin E (Faramarzi et al., 2010).

Fig. 2b shows TGA graphs of XG, SL, OGs, and E-OGs. XG showed an initial weight loss of approximately 10% due to the evaporation of moisture and volatile matter. Subsequently, a dominant degradation process occurred, resulting in a weight loss of about 45% in the temperature range of 250–300 °C (Sethi, SaruchiKaith, Kaur, Sharma, & Kumar, 2020). SL showed weight loss in the temperature range of 200–400 °C, which appears to be due to its complex composition. The decomposition temperature of SL was approximately 280 °C, with a weight loss of about 70% as the temperature reached 400 °C (Li, Wu, Wang, & Liu, 2013). OGs showed significant weight loss of approximately 100% in the temperature range of 300–450 °C. In contrast, E-OGs exhibited a two-step degradation process. The first stage resulted in a weight loss of 7% over a temperature range of 220–320 °C, while the second stage resulted in a weight loss of approximately 85% over a temperature range of 320–450 °C. In comparison, OGs and E-OGs showed a decomposition process at a higher temperature than XG and SL. This increased thermal stability can be attributed to the presence of hydrogen bonds and electrostatic interactions between XG and SL, which are known to contribute to higher thermal stability (Sharma et al., 2015).

3.3. Oxidative stability

According to the Schaal oven method, the quality of lipids at 60 °C for one day is the same as that at room temperature for one month (Abou-Gharbia et al., 1996). PV, ρ-AV, and TOTOX of the OGs were measured at 60 °C for 12 days and compared to those of the commercially available butter and soybean oil (Fig. 3). PV and ρ-AV indicate the formation of primary and secondary oxidation products (Li et al., 2019). The PV of soybean oil increased rapidly to 88.41 ± 2.93 mmol/kg after 10 days of storage which is almost eight times as high as that of OGs (11.46 ± 0.57 mmol/kg). The PV of butter showed the lowest ranges from 0.47 ± 0.29 mmol/kg to 2.23 ± 0.28 mmol/kg. The ρ-AV of soybean oil was gradually increased with storage time ranging from 9.69 ± 0.14 to 51.17 ± 0.84, while the ρ-AV of OGs and butter ranged from 8.54 ± 0.48 to 10.99 ± 0.14 and from 0.63 ± 0.45 to 3.47 ± 0.98, respectively. This phenomenon may be due to the entrapment of soybean oil in the oleogel structure formed by XG and SL, which reduces the interaction with air and retards oxidation (Kamali, Sahari, Barzegar, & Ahmadi Gavlighi, 2019). This network structure may act as a physical barrier, effectively blocking oil droplets from direct exposure to atmospheric oxygen. Similar results were reported that the oxidative stability of oleogels was enhanced by the adsorption of oleogelator at the surface of oil dropets (Khouryieh, Puli, Williams, & Aramouni, 2015).

Fig. 3c shows TOTOX results calculated from PV and ρ-AV values, which serve as a more comprehensive indicator of overall oil quality. The TOTOX values of OGs were significantly lower than those of pure soybean oil. Low TOTOX values indicate good oil quality as they reflect reduced levels of primary and secondary oxidation products. The TOTOX of OGs was lower than that of pure soybean oil, meaning better oil quality. The TOTOX of OGs and soybean oil reached 42.88 ± 1.75 and 184.65 ± 6.81, respectively, at 12 days of storage. On the other hand, commercially available butter contains saturated fatty acids with almost no double bonds at unstable positions in the molecular structure of fatty acids, and thus has the lowest oxidation stability (Zaldman, Kisilev, Sasson, & Garti, 1988). Besides, the commercially available butter contains more natural antioxidants, such as vitamin E and carotenoids. These antioxidants act to inhibit or retard oxidation, improving the oxidative stability of butter (Khan et al., 2019). OGs exhibit strong oxidation stability even without natural antioxidants, and when compounds such as vitamin E are added, they can exhibit superior oxidative stability compared to butter. Therefore, OGs are emerging as a promising alternative or complement to butter. In other research, oleogelation enhanced the oxidative stability of corn oil, similar to that

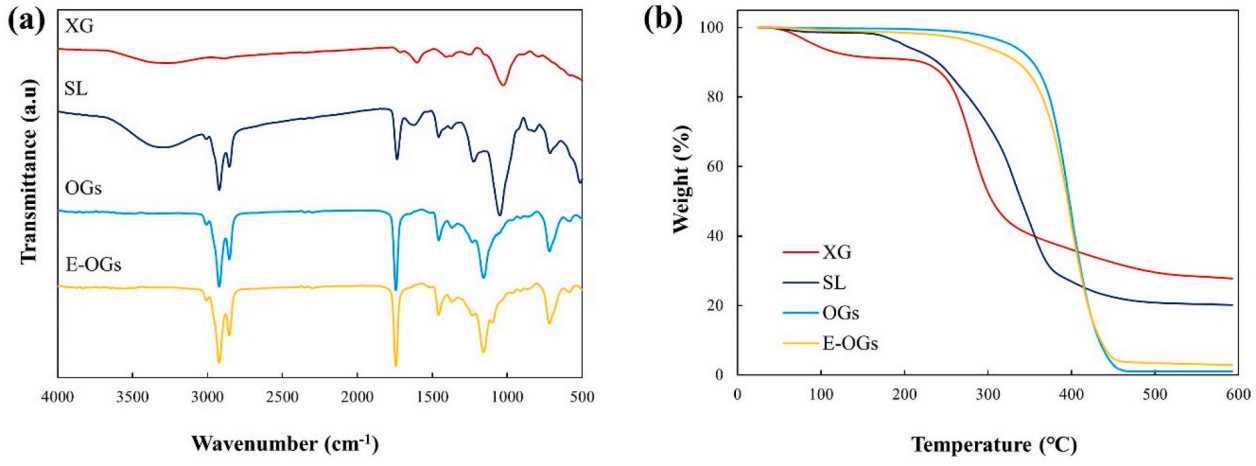

Fig. 2. FT-IR (a) and TGA (b) spectra of XG, SL, OGs, and E-OGs.

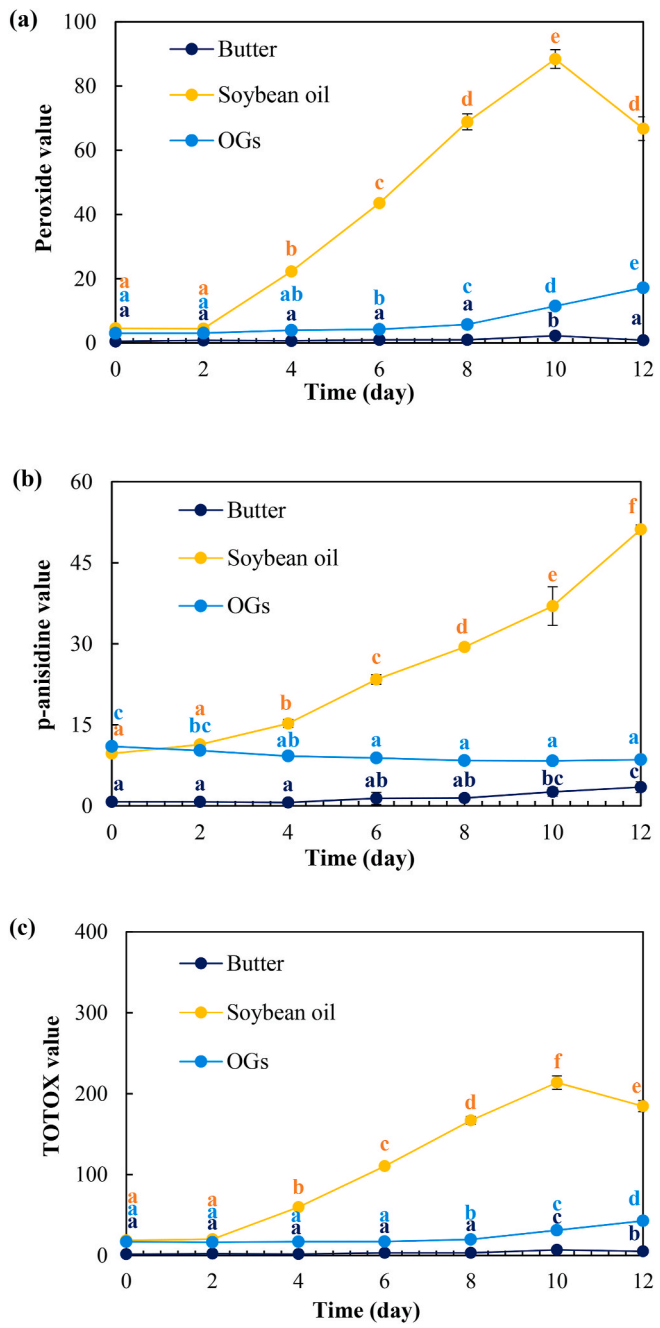

Fig. 3. Peroxide value (a), ρ-anisidine value (b), and total oxidation (TOTOX) value (c) as oxidative stability of butter, soybean oil, and oleogels.

of the addition of curcumin as an antioxidant (Li et al., 2019). Su et al. (2023) prepared emulsion-templated oleogels with egg-white protein (EWP) and XG as an oleogelator and found that the oxidation stability improved depending on the concentration of EWP and XG. The oleogelator was adsorbed to the outside of oil droplets and prevents the oil droplets fromcoming into contact with oxygen, delaying the oxidation process. Zhuang, Gaudino, Clark, and Acevedo (2021) also reported the oxidative stability of emulsion-based oleogels structured with SL. The fibrillar network of SL may result from delayed oxidation or reduced molecular collisions through the physical entrapment of oil.

3.4. *In vitro lipid digestion*

Lipid digestion profiles were investigated by monitoring the release of FFAs from E-OGs, OGs, and butter during *in vitro* digestion. As shown in Fig. 4a, FFAs release increased rapidly during the first few minutes of digestion and then increased gradually. Additionally, E-OGs and OGs released more FFAs than butter. E-OGs and OGs released 85.27% ± 2.33% and 78.40% ± 6.94% of FFAs, respectively, whereas butter released 66.00% ± 1.10% of FFAs after digestion for 120 min. This result may be because the lipid droplets in E-OGs and OGs provide a higher surface area to interact with enzymes. E-OGs and OGs are therefore more susceptible to enzymatic hydrolysis than butter (Zhang et al., 2022). Additionally, it is plausible that amphiphilic XG molecules play a role in the generation of mixed micelles during digestion. This process could potentially improve the ability to solubilize FFAs (Wilde & Chu, 2011), indicating that oleogelation does not negatively affect the digestion of triacylglycerols present in soybean oil. It may promote digestion (Shuai et al., 2023). Wang et al. (2022) used soybean oil body (high in unsaturated fatty acids) with milk fat (high in saturated fatty acid) instead of ice cream and reported that the release of FFAs increased significantly with more substitution of unsaturated fatty acids for saturated fatty acids. The microstructure of E-OGs during *in vitro* digestion is shown in Fig. 4c. Oil phase and XG were stained using Nile red and Calcofluor White fluorescent dyes, and spherical particles were initially seen due to the emulsion template. The SSF showed stable spherical particles, whereas the XG layer was slightly separated under the SGF. After SIF digestion, E-OGs showed an amorphous appearance as a result of lipid degradation by the action of lipase and bile salts as droplet agglomeration (Park et al., 2019). These findings were further corroborated by visual comparison of samples prepared using dyed soybean oil (containing Nile red) and XG (containing Calcofluor White) before and after digestion (Fig. 4b). The samples appeared homogeneous before digestion, but the XG layer (blue color) was precipitated after digestion. In addition, lipolysis was observed due to the enzymatic action of lipase and bile salts, and the separation of the soybean oil layer (red color) was observed. These observations are consistent with the microstructural changes shown in Fig. 4c during *in vitro* digestion. The bioaccessibility of vitamin E and E-OGs was investigated (Supplementary Fig. S1). The bioaccessibility of E-OGs was 75.91% ± 0.23% after 6 h of digestion, while pure vitamin E showed a bioaccessibility of 2.71% ± 0.66% after digestion. This phenomenon is consistent with the findings of Zhang, Jiang, Ling, Ouyang, and Wang (2021), who reported a similar trend with curcumin encapsulated using XG, showing higher release in SGF and SIF compared to pure curcumin. E-OGs containing SL were shown to enhance the solubility of vitamin E by interacting with the interface of oil droplets (Kateh Shamshiri, Momtazi-Borojeni, Khodabandeh Shahraky & Rahimi, 2019).

3.5. *The application of E-OGs in pound cakes*

Prepared pound cakes are designated to E-OGs-0 (100% butter), E-OGs-20, E-OGs-40, E-OGs-60, E-OGs-80, and E-OGs-100 based on the content of E-OGs. To evaluate E-OGs as a commercial butter replacer for pound cakes, the texture properties, structure, and porosity of pound cakes were determined. As shown in Table 2, the hardness and chewiness of the pound cake had a positive effect when E-OGs were replaced with butter. Hardness is the force with which food reaches a given deformation (Psimouli & Oreopoulou, 2013). The increase in hardness value means that the cake became harder and more resistant to deformation when E-OGs were used as a butter substitute. This change in hardness can significantly affect the sensory experience of consuming pound cake because it requires greater force during mastication and chewing. Chewiness is the energy required to chew food before swallowing it (Di Monaco, Cavella, & Masi, 2008). Increasing these parameters requires more force for mastication and has been reported to negatively affect food (Pan et al., 2021).

Micro-computed tomographic (micro-CT) analysis was performed to evaluate the microstructure and porosity of the pound cake. In micro-CT analysis, the pores of the pound cake appear black, and the denser they

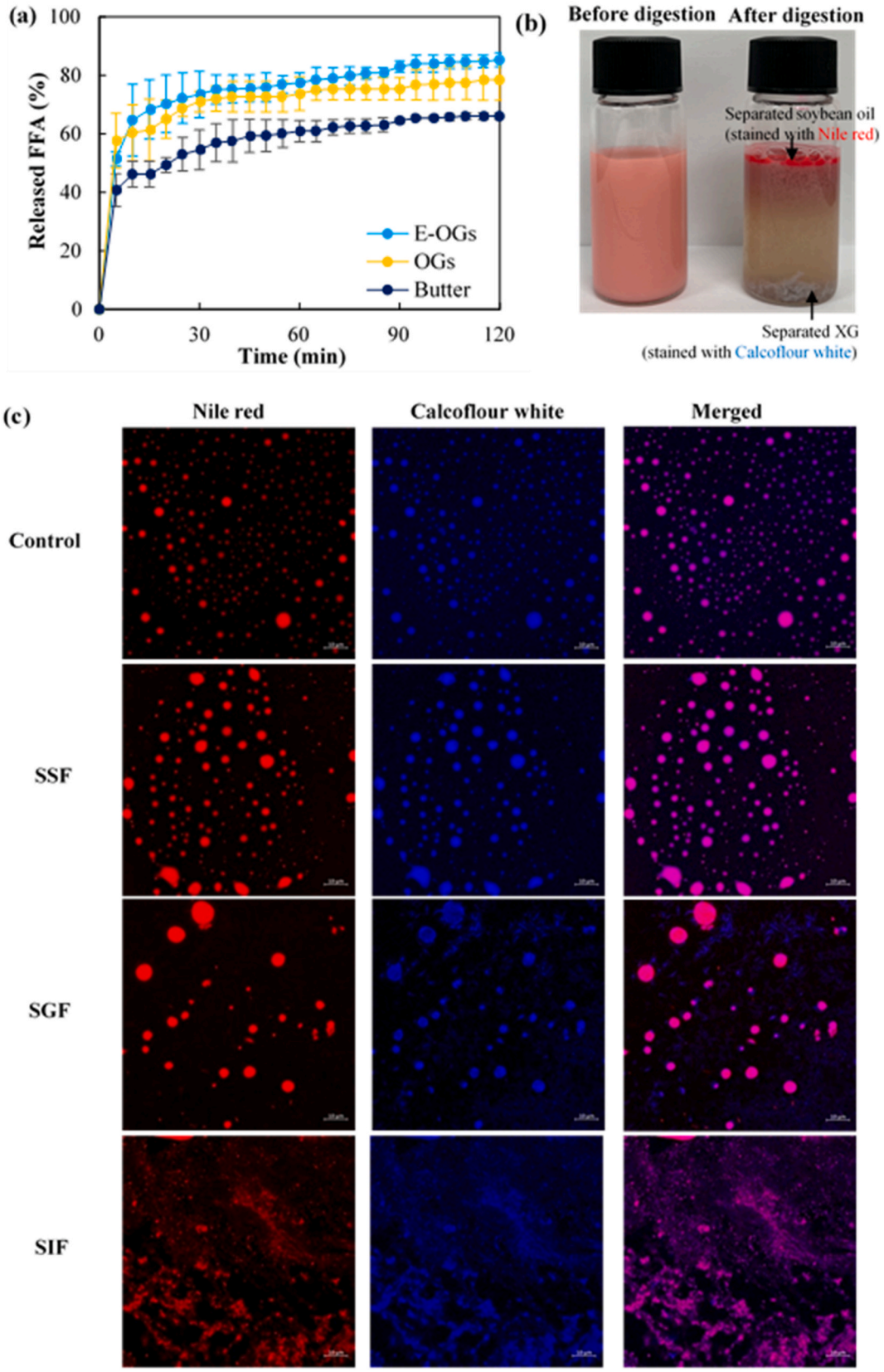

Fig. 4. Released free fatty acid amounts from E-OGs, OGs, and commercial butter in small intestinal fluid (a), digital photographs (b), and confocal laser scanning microscope (CLSM) images (c) of E-OGs before and after *in vitro* lipid digestion.

Table 2
Changes in texture parameters of pound cakes prepared with various concentrations of E-OG.

Day	Sample	Hardness (N)	Adhesiveness (mJ)	Springiness	Chewiness (N)	Cohesiveness
0	E-OGs-0	$9.73 \pm 1.33^{b,A,*}$	$0.36 \pm 0.07^{a,A}$	$0.68 \pm 0.10^{ab,B}$	$1.76 \pm 0.60^{b,A}$	$0.26 \pm 0.04^{b,A}$
	E-OGs-20	$9.77 \pm 0.67^{b,A}$	$0.50 \pm 0.07^{ab,A}$	$0.71 \pm 0.02^{bc,B}$	$1.77 \pm 0.20^{b,A}$	$0.25 \pm 0.03^{b,A}$
	E-OGs-40	$9.55 \pm 1.05^{b,A}$	$0.48 \pm 0.09^{ab,A}$	$0.72 \pm 0.03^{bc,B}$	$1.82 \pm 0.30^{b,B}$	$0.26 \pm 0.02^{b,B}$
	E-OGs-60	$9.07 \pm 1.33^{ab,A}$	$0.46 \pm 0.07^{ab,A}$	$0.77 \pm 0.03^{c,B}$	$2.00 \pm 0.42^{b,B}$	$0.28 \pm 0.01^{b,B}$
	E-OGs-80	$8.76 \pm 0.40^{ab,A}$	$0.45 \pm 0.05^{ab,A}$	$0.62 \pm 0.05^{a,A}$	$0.99 \pm 0.20^{a,A}$	$0.18 \pm 0.03^{a,A}$
	E-OGs-100	$7.95 \pm 0.58^{a,A}$	$0.61 \pm 0.29^{b,A}$	$0.61 \pm 0.03^{a,A}$	$0.94 \pm 0.21^{a,A}$	$0.22 \pm 0.08^{a,A}$
3	E-OGs-0	$15.67 \pm 0.87^{c,B}$	$0.47 \pm 0.19^{ab,B}$	$0.72 \pm 0.03^{b,B}$	$2.38 \pm 0.29^{c,B}$	$0.22 \pm 0.03^{c,A}$
	E-OGs-20	$15.40 \pm 0.53^{bc,B}$	$0.36 \pm 0.12^{a,B}$	$0.72 \pm 0.05^{b,B}$	$1.82 \pm 0.43^{b,A}$	$0.18 \pm 0.04^{b,A}$
	E-OGs-40	$15.33 \pm 0.59^{bc,B}$	$0.42 \pm 0.10^{a,B}$	$0.66 \pm 0.05^{b,B}$	$2.10 \pm 0.42^{bc,B}$	$0.19 \pm 0.04^{bc,B}$
	E-OGs-60	$15.41 \pm 0.54^{bc,B}$	$0.89 \pm 0.36^{b,B}$	$0.60 \pm 0.06^{a,A}$	$1.23 \pm 0.34^{a,A}$	$0.16 \pm 0.05^{a,A}$
	E-OGs-80	$14.86 \pm 0.41^{ab,B}$	$0.91 \pm 0.52^{b,A}$	$0.58 \pm 0.04^{a,A}$	$1.05 \pm 0.14^{a,A}$	$0.12 \pm 0.01^{a,A}$
	E-OGs-100	$14.68 \pm 0.31^{a,B}$	$0.61 \pm 0.29^{ab,A}$	$0.58 \pm 0.06^{a,A}$	$0.99 \pm 0.23^{a,A}$	$0.12 \pm 0.02^{a,A}$
7	E-OGs-0	$19.83 \pm 0.80^{b,C}$	$0.91 \pm 0.26^{b,C}$	$0.57 \pm 0.03^{a,A}$	$1.65 \pm 0.33^{a,A}$	$0.17 \pm 0.07^{a,B}$
	E-OGs-20	$20.18 \pm 0.77^{b,C}$	$0.78 \pm 0.14^{b,C}$	$0.61 \pm 0.04^{a,A}$	$1.59 \pm 0.34^{a,A}$	$0.13 \pm 0.02^{a,A}$
	E-OGs-40	$20.22 \pm 0.62^{b,C}$	$0.73 \pm 0.12^{ab,C}$	$0.56 \pm 0.07^{a,A}$	$1.31 \pm 0.30^{a,A}$	$0.12 \pm 0.02^{a,A}$
	E-OGs-60	$19.85 \pm 0.45^{b,C}$	$0.72 \pm 0.17^{ab,AB}$	$0.62 \pm 0.07^{a,A}$	$1.33 \pm 0.23^{a,A}$	$0.13 \pm 0.05^{a,A}$
	E-OGs-80	$18.74 \pm 0.66^{a,C}$	$0.51 \pm 0.21^{a,A}$	$0.62 \pm 0.06^{a,A}$	$1.74 \pm 0.47^{a,B}$	$0.19 \pm 0.06^{a,B}$
	E-OGs-100	$18.77 \pm 0.50^{a,C}$	$0.66 \pm 0.16^{ab,A}$	$0.61 \pm 0.06^{a,A}$	$1.40 \pm 0.26^{a,B}$	$0.15 \pm 0.05^{a,B}$

* Different letters (a–c) and (A–C) in the same column indicate a significant difference in each texture parameter among the sample and time, respectively ($p < 0.05$).

are, the brighter they appear due to the scattering of X-rays (Meng, Qi, Guo, Wang, & Liu, 2018). As shown in Fig. 5, the micro-CT image of the pound cake prepared with butter showed brighter areas. As the E-OGs amount increased, the bright area decreased and small pores were uniformly distributed. The porosity of pound cake was in good agreement shown in Fig. 5. A significant ($p < 0.05$) increase of porosity was found with increasing replacement of E-OGs from 62.45% ± 1.88% for E-OGs-0 to 70.73% ± 1.56% for E-OGs-100. The increase in porosity of the pound cake when substituting E-OGs can be attributed to the emulsifiers in E-OGs (Malvano, Laudisio, Albanese, d'Amore, & Marra, 2022), which creates small and evenly distributed pores throughout the pound cake, ultimately increasing the overall porosity. A similar

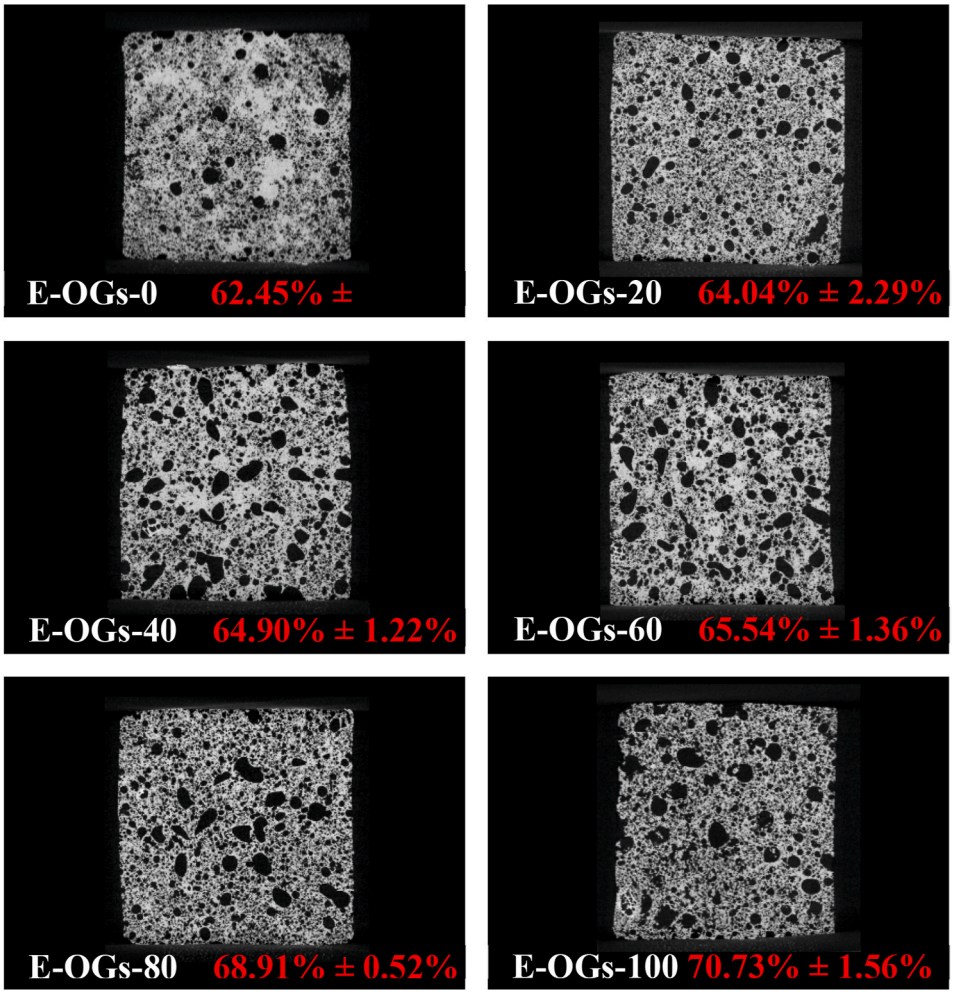

Fig. 5. Micro-CT tomographical 2-dimension (a) images of pound cakes prepared with various concentrations of E-OGs as a replacement of butter.

phenomenon was also reported by Ye, Li, Lo, Fu, and Cao (2019), who applied ethylcellulose oleogel to bread and found that it increased the porosity of bread compared to bread using commercial solid fats.

The properties of OGs, which are designed to structure oils, play an important role in capturing the numerous air bubbles within the pound cake matrix. This structural arrangement not only improves the integration and stabilization of finer bubbles but also results in the development of a final product with uniformly distributed pores (Patel & Dewettinck, 2016). These unique properties also contribute significantly to creating cakes with a light and soft texture, perfectly matched by the reduced hardness and chewiness compared to the cake prepared with butter. Additionally, as shown in Table 2, the persistent springiness observed in the cake prepared with E-OGs-100, can be attributed to the substantial elastic modulus and loss modulus exhibited by OGs (see Fig. 1b). This persistent springiness serves as a testament to the stability of OGs and maintains the structural integrity and textural quality of the cake over a long period.

4. Conclusion

E-OGs were successfully prepared with XG and SL with high OBC and rheology properties and good oxidative stability. Optimized E-OGs were evaluated as a solid fat (butter) replacer to make a pound cake. The results showed that replacing butter with E-OGs reduced the hardness of pound cake, resulting in a softer texture. Additionally, the overall porosity of the pound cake increased, meaning there were more air cells within the cake structure. These findings are important because they show that E-OGs can effectively replace butter in pound cake recipes without compromising the quality of the final product. The function of E-OGs as a butter replacer was studied by comparing texture and porosity changes in cake products. By replacing butter with E-OGs, the hardness of the pound cake decreased from 9.73 ± 1.33 N to 7.95 ± 0.58 N and the total porosity increased from 63.93% ± 3.87%–70.67% ± 4.03%. This result is a soft pound cake with improved overall appeal, and growing consumer preference. Most of the air cells are much smaller in size and evenly distributed in the pound cake prepared with E-OGs. Therefore, E-OGs was a viable replacement for butter to create high-quality bakery products with small air cells and uniform distribution throughout the pound cake. As a result, the texture is usually uniform, light, and fluffy. This quality is highly desirable for pound cakes as it enhances the overall sensory experience and provides a pleasant texture and attractive appearance. Further research is needed to how to incorporate functional materials into OG to enhance their functions.

CRediT authorship contribution statement

Su Jung Hong: Conceptualization, Data curation, Formal analysis, Funding acquisition, Investigation, Visualization, Writing – original draft. **Gye Hwa Shin:** Supervision, Writing – review & editing. **Jun Tae Kim:** Conceptualization, Supervision, Writing – review & editing.

Declaration of competing interest

The authors declare that they have no known competing financial interests or personal relationships that could have appeared to influence the work reported in this paper.

Data availability

The authors do not have permission to share data.

Acknowledgements

This research was supported by Samyang Igeon (以建) Scholarship Foundation.

Appendix A. Supplementary data

Supplementary data to this article can be found online at https://doi.org/10.1016/j.fbio.2023.103505.

References

Abou-Gharbia, H. A., Shahidi, F., Shehata, A. A. Y., & Youssef, M. M. (1996). Oxidative stability of extracted sesame oil from raw and processed seeds. *Journal of Food Lipids, 3*(1), 59–72. https://doi.org/10.1111/j.1745-4522.1996.tb00054.x

Alloncle, M., & Doublier, J. L. (1991). Viscoelastic properties of maize starch/hydrocolloid pastes and gels. *Topics in Catalysis, 5*(5), 455–467. https://doi.org/10.1016/S0268-005X(09)80104-5

Balcaen, M., Steyls, J., Schoeppe, A., Nelis, V., & Van der Meeren, P. (2021). Phosphatidylcholine-depleted lecithin: A clean-label low-HLB emulsifier to replace PGPR in w/o and w/o/w emulsions. *Journal of Colloid and Interface Science, 581*, 836–846. https://doi.org/10.1016/j.jcis.2020.07.149

Blake, A. I., & Marangoni, A. G. (2015). The use of cooling rate to engineer the microstructure and oil binding capacity of wax crystal networks. *Food Biophysics, 10*(4), 456–465. https://doi.org/10.1007/s11483-015-9409-0

Brodkorb, A., Egger, L., Alminger, M., Alvito, P., Assunção, R., Ballance, S., et al. (2019). INFOGEST static *in vitro* simulation of gastrointestinal food digestion. *Nature Protocols, 14*(4), 991–1014. https://doi.org/10.1038/s41596-018-0119-1

Cai, Y., Deng, X., Liu, T., Zhao, M., Zhao, Q., & Chen, S. (2018). Effect of xanthan gum on walnut protein/xanthan gum mixtures, interfacial adsorption, and emulsion properties. *Food Hydrocolloids, 79*, 391–398. https://doi.org/10.1016/j.foodhyd.2018.01.006

Chuesiang, P., Zhang, J., Choi, E., Yoon, I.-S., Kim, J. T., & Shin, G. H. (2022). Observation of curcumin-loaded hydroxypropyl methylcellulose (HPMC) oleogels under in vitro lipid digestion and in situ intestinal absorption in rats. *International Journal of Biological Macromolecules, 208*, 520–529. https://doi.org/10.1016/j.ijbiomac.2022.03.120

Clausse, D., Lanoisellé, J. L., Pezron, I., & Saleh, K. (2018). Formulation of a water-in-oil emulsion encapsulating polysaccharides to improve the efficiency of spraying of plant protection products. *Colloids and Surfaces A: Physicochemical and Engineering Aspects, 536*, 96–103. https://doi.org/10.1016/j.colsurfa.2017.07.032

Demirkesen, I., & Mert, B. (2020). Recent developments of oleogel utilizations in bakery products. *Critical Reviews in Food Science and Nutrition, 60*(14), 2460–2479. https://doi.org/10.1080/10408398.2019.1649243

Di Monaco, R., Cavella, S., & Masi, P. (2008). Predicting sensory cohesiveness, hardness and springiness of solid foods from instrumental measurements. *Journal of Texture Studies, 39*(2), 129–149. https://doi.org/10.1111/j.1745-4603.2008.00134.x

Erramreddy, V. V., Tu, S., & Ghosh, S. (2017). Rheological reversibility and long-term stability of repulsive and attractive nanoemulsion gels. *RSC Advances, 7*(75), 47818–47832. https://doi.org/10.1039/C7RA09605D

Faramarzi, M. A., Naghibzadeh, M., Amani, A., Amini, M., Esmaeilzadeh, E., & Mottaghi-Dastjerdi, N. (2010). An insight into the interactions between-tocopherol and chitosan in ultrasound-prepared nanoparticles. *Journal of Nanomaterials, 44*. https://doi.org/10.1155/2010/818717, 2010.

Goh, K. Y., Ching, Y. C., Ng, M. H., Chuah, C. H., & Julaihi, S. B. J. (2022). Microfibrillated cellulose-reinforced alginate microbeads for delivery of palm-based vitamin E: Characterizations and *in vitro* evaluation. *Journal of Drug Delivery Science and Technology, 71*, Article 103324. https://doi.org/10.1016/j.jddst.2022.103324

Hong, S. J., Garcia, C. V., Park, S. J., Shin, G. H., & Kim, J. T. (2019). Retardation of curcumin degradation under various storage conditions via turmeric extract-loaded nanoemulsion system. *LWT-Food Science & Technology, 100*, 175–182. https://doi.org/10.1016/j.lwt.2018.10.056

Hong, S. J., Garcia, C. V., Shin, G. H., & Kim, J. T. (2022). Enhanced bioaccessibility and stability of iron through W/O/W double emulsion-based solid lipid nanoparticles and coating with water-soluble chitosan. *International Journal of Biological Macromolecules, 209*, 895–903. https://doi.org/10.1016/j.ijbiomac.2022.04.066

Huang, X., Kakuda, Y., & Cui, W. (2001). Hydrocolloids in emulsions: Particle size distribution and interfacial activity. *Food Hydrocolloids, 15*(4–6), 533–542. https://doi.org/10.1016/S0268-005X(01)00091-1

Jafarifar, Z., Rezaie, M., Sharifan, P., Jahani, V., Daneshmand, S., Ghazizadeh, H., et al. (2022). Preparation and characterization of nanostructured lipid carrier (NLC) and nanoemulsion containing vitamin D3. *Applied Biochemistry and Biotechnology, 194*(2), 914–929. https://doi.org/10.1007/s12010-021-03656-z

Kamali, E., Sahari, M. A., Barzegar, M., & Ahmadi Gavlighi, H. (2019). Novel oleogel formulation based on amaranth oil: Physicochemical characterization. *Food Science and Nutrition, 7*(6), 1986–1996. https://doi.org/10.1002/fsn3.1018

Kateh Shamshiri, M., Momtazi-Borojeni, A. A., Khodabandeh Shahraky, M., & Rahimi, F. (2019). Lecithin soybean phospholipid nano-transfersomes as potential carriers for transdermal delivery of the human growth hormone. *Journal of Cellular Biochemistry, 120*(6), 9023–9033. https://doi.org/10.1002/jcb.28176

Khan, I. T., Nadeem, M., Imran, M., Ullah, R., Ajmal, M., & Jaspal, M. H. (2019). Antioxidant properties of milk and dairy products: A comprehensive review of the current knowledge. *Lipids in Health and Disease, 18*, 1–13. https://doi.org/10.1186/s12944-019-0969-8

Khouryieh, H., Puli, G., Williams, K., & Aramouni, F. (2015). Effects of xanthan-locust bean gum mixtures on the physicochemical properties and oxidative stability of whey protein stabilised oil-in-water emulsions. *Food Chemistry, 167*, 340–348. https://doi.org/10.1016/j.foodchem.2014.07.009

Kim, C., & Yoo, B. (2006). Rheological properties of rice starch-xanthan gum mixtures. *Journal of Food Engineering, 75*(1), 120–128. https://doi.org/10.1016/j.jfoodeng.2005.04.002

Li, L., Wan, W., Cheng, W., Liu, G., & Han, L. (2019). Oxidatively stable curcumin-loaded oleogels structured by β-sitosterol and lecithin: Physical characteristics and release behaviour *in vitro*. *International Journal of Food Science and Technology, 54*(7), 2502–2510. https://doi.org/10.1111/ijfs.14208

Li, W., Wu, Y., Wang, X., & Liu, W. (2013). Study of soybean lecithin as multifunctional lubricating additives. *Industrial Lubrication & Tribology, 65*(6), 466–471. https://doi.org/10.1108/ILT-06-2011-0050

Li, J., Xi, Y., Wu, L., & Zhang, H. (2023). Preparation, characterization and *in vitro* digestion of bamboo shoot protein/soybean protein isolate based-oleogels by emulsion-templated approach. *Food Hydrocolloids, 136*, Article 108310. https://doi.org/10.1016/j.foodhyd.2022.108310

Malvano, F., Laudisio, M., Albanese, D., d'Amore, M., & Marra, F. (2022). Olive oil-based oleogel as fat replacer in a sponge cake: A comparative study and optimization. *Foods, 11*(17), 2643. https://doi.org/10.3390/foods11172643

Manosso, L. M., Camargo, A., Dafre, A. L., & Rodrigues, A. L. S. (2022). Vitamin E for the management of major depressive disorder: Possible role of the anti-inflammatory and antioxidant systems. *Nutritional Neuroscience, 25*(6), 1310–1324. https://doi.org/10.1080/1028415X.2020.1853417

Meng, Z., Guo, Y., Wang, Y., & Liu, Y. (2019). Oleogels from sodium stearoyl lactylate-based lamellar crystals: Structural characterization and bread application. *Food Chemistry, 292*, 134–142. https://doi.org/10.1016/j.foodchem.2018.11.042

Meng, Z., Qi, K., Guo, Y., Wang, Y., & Liu, Y. (2018). Macro-micro structure characterization and molecular properties of emulsion-templated polysaccharide oleogels. *Food Hydrocolloids, 77*, 17–29. https://doi.org/10.1016/j.foodhyd.2017.09.006

Michał, W., Ewa, D., & Tomasz, C. (2015). Lecithin-based wet chemical precipitation of hydroxyapatite nanoparticles. *Colloid and Polymer Science, 293*(5), 1561–1568. https://doi.org/10.1007/s00396-015-3557-0

Minekus, M., Alminger, M., Alvito, P., Ballance, S., Bohn, T., Bourlieu, C., et al. (2014). A standardised static *in vitro* digestion method suitable for food–an international consensus. *Food & Function, 5*(6), 1113–1124. https://doi.org/10.1039/C3FO60702J

Mirhosseini, H., Tan, C. P., Hamid, N. S. A., & Yusof, S. (2008). Effect of Arabic gum, xanthan gum and orange oil contents on ζ-potential, conductivity, stability, size index and pH of orange beverage emulsion. *Colloids and Surfaces A: Physicochemical and Engineering Aspects, 315*(1–3), 47–56. https://doi.org/10.1016/j.colsurfa.2007.07.007

Oh, I., Lee, J., Lee, H. G., & Lee, S. (2019). Feasibility of hydroxypropyl methylcellulose oleogel as an animal fat replacer for meat patties. *Food Research International, 122*, 566–572. https://doi.org/10.1016/j.foodres.2019.01.012

Pan, H., Xu, X., Qian, Z., Cheng, H., Shen, X., Chen, S., et al. (2021). Xanthan gum-assisted fabrication of stable emulsion-based oleogel structured with gelatin and proanthocyanidins. *Food Hydrocolloids, 115*, Article 106596. https://doi.org/10.1016/j.foodhyd.2021.106596

Park, S. J., Garcia, C. V., Shin, G. H., & Kim, J. T. (2018). Improvement of curcuminoid bioaccessibility from turmeric by a nanostructured lipid carrier system. *Food Chemistry, 251*, 51–57. https://doi.org/10.1016/j.foodchem.2018.01.071

Park, S. J., Hong, S. J., Garcia, C. V., Lee, S. B., Shin, G. H., & Kim, J. T. (2019). Stability evaluation of turmeric extract nanoemulsion powder after application in milk as a food model. *Journal of Food Engineering, 259*, 12–20. https://doi.org/10.1016/j.jfoodeng.2019.04.011

Patel, A. R., & Dewettinck, K. (2016). Edible oil structuring: An overview and recent updates. *Food & Function, 7*(1), 20–29. https://doi.org/10.1039/c5fo01006c

Patel, A. R., Rajarethinem, P. S., Cludts, N., Lewille, B., De Vos, W. H., Lesaffer, A., et al. (2015). Biopolymer-based structuring of liquid oil into soft solids and oleogels using water-continuous emulsions as templates. *Langmuir, 31*(7), 2065–2073. https://doi.org/10.1021/la502829u

Psimouli, V., & Oreopoulou, V. (2013). The effect of fat replacers on batter and cake properties. *Journal of Food Science, 78*(10), C1495–C1502. https://doi.org/10.1111/1750-3841.12235

Pușcaș, A., Mureșan, V., Socaciu, C., & Muste, S. (2020). Oleogels in food: A review of current and potential applications. *Foods, 9*(1), 70. https://doi.org/10.3390/foods9010070

Said, M., Haq, B., Shehri, D. Al, Rahman, M. M., Muhammed, N. S., & Mahmoud, M. (2021). Modification of xanthan gum for a high-temperature and high-salinity reservoir. *Polymers, 13*(23), 1–13. https://doi.org/10.3390/polym13234212

Sapiejka, E., Krzyżanowska-Jankowska, P., Wenska-Chyży, E., Szczepanik, M., Walkowiak, D., Cofta, S., et al. (2018). Vitamin E status and its determinants in patients with cystic fibrosis. *Advances in Medical Sciences, 63*(2), 341–346. https://doi.org/10.1016/j.advms.2018.04.001

Sethi, S., Saruchi, Kaith, B. S., Kaur, M., Sharma, N., & Kumar, V. (2020). Cross-linked xanthan gum–starch hydrogels as promising materials for controlled drug delivery. *Cellulose, 27*(8), 4565–4589. https://doi.org/10.1007/s10570-020-03082-0

Sharma, K., Kumar, V., Kaith, B. S., Som, S., Kumar, V., Pandey, A., et al. (2015). Synthesis of biodegradable gum ghatti based poly(methacrylic acid-aniline) conducting IPN hydrogel for controlled release of amoxicillin trihydrate. *Industrial & Engineering Chemistry Research, 54*(7), 1982–1991. https://doi.org/10.1021/ie5044743

Shuai, X., McClements, D. J., Geng, Q., Dai, T., Ruan, R., Du, L., et al. (2023). Macadamia oil-based oleogels as cocoa butter alternatives: Physical properties, oxidative stability, lipolysis, and application. *Food Research International, 172*, Article 113098. https://doi.org/10.1016/j.foodres.2023.113098

Siyal, F. J., Memon, Z., Siddiqui, R. A., Aslam, Z., Nisar, U., Imad, R., et al. (2020). Eugenol and liposome-based nanocarriers loaded with eugenol protect against anxiolytic disorder via down regulation of neurokinin-1 receptors in mice. *Pakistan journal of pharmaceutical sciences, 33*(5), 2275–2284. https://doi.org/10.36721/PJPS.2020.33.5.SUP.2275-2284.1

Su, Y., Zhang, W., Liu, R., Chang, C., Li, J., Xiong, W., et al. (2023). Emulsion-templated liquid oil structuring with egg white protein microgel-xanthan gum. *Foods, 12*(9), 1–16. https://doi.org/10.3390/foods12091884

Vázquez, E., Piguillem, S., Rubio, S., Díaz, J., Baldoni, H., Vega, E., et al. (2020). Structural analysis of xanthan gum-FE (III) capsules. *Academic Journal of Chemistry, 5*(54), 31–40. https://doi.org/10.32861/ajc.54.31.40

Violi, F., Nocella, C., Loffredo, L., Carnevale, R., & Pignatelli, P. (2022). Interventional study with vitamin E in cardiovascular disease and meta-analysis. *Free Radical Biology and Medicine, 178*, 26–41. https://doi.org/10.1016/j.freeradbiomed.2021.11.027

Wang, Q., Espert, M., Larrea, V., Quiles, A., Salvador, A., & Sanz, T. (2023). Comparison of different indirect approaches to design edible oleogels based on cellulose ethers. *Food Hydrocolloids, 134*, Article 108007. https://doi.org/10.1016/j.foodhyd.2022.108007

Wang, W., Wang, M., Xu, C., Liu, Z., Gu, L., Ma, J., et al. (2022). Effects of soybean oil body as a milk fat substitute on ice cream: Physicochemical, sensory and digestive properties. *Foods, 11*(10), 1504. https://doi.org/10.3390/foods11101504

Wang, M., Yan, W., Zhou, Y., Fan, L., Liu, Y., & Li, J. (2021). Progress in the application of lecithins in water-in-oil emulsions. *Trends in Food Science and Technology, 118*, 388–398. https://doi.org/10.1016/j.tifs.2021.10.019 (PA).

Wilde, P. J., & Chu, B. S. (2011). Interfacial & colloidal aspects of lipid digestion. *Advances in Colloid and Interface Science, 165*(1), 14–22. https://doi.org/10.1016/j.cis.2011.02.004

Xing, X., Chitrakar, B., Hati, S., Xie, S., Li, H., Li, C., et al. (2022). Development of black fungus-based 3D printed foods as dysphagia diet: Effect of gums incorporation. *Food Hydrocolloids, 123*, Article 107173. https://doi.org/10.1016/j.foodhyd.2021.107173

Ye, X., Li, P., Lo, Y. M., Fu, H., & Cao, Y. (2019). Development of novel shortenings structured by ethylcellulose oleogels. *Journal of Food Science, 84*(6), 1456–1464. https://doi.org/10.1111/1750-3841.14615

Zaldman, B., Kisilev, A., Sasson, Y., & Garti, N. (1988). Double bond oxidation of unsaturated fatty acids. *Journal of the American Oil Chemists' Society, 65*, 611–615. https://doi.org/10.1007/BF02540689

Zhang, J., Chuesiang, P., Kim, J. T., & Shin, G. H. (2022). The role of nanostructured lipid carriers and type of biopolymers on the lipid digestion and release rate of curcumin from curcumin-loaded oleogels. *Food Chemistry, 392*, Article 133306. https://doi.org/10.1016/j.foodchem.2022.133306

Zhang, D., Jiang, F., Ling, J., Ouyang, X., & Wang, Y.-G. (2021). Delivery of curcumin using a zein-xanthan gum nanocomplex: Fabrication, characterization, and *in vitro* release properties. *Colloids and Surfaces B: Biointerfaces, 204*, Article 111827. https://doi.org/10.1016/j.colsurfb.2021.111827

Zhao, Q., Zhao, M., Yang, B., & Cui, C. (2009). Effect of xanthan gum on the physical properties and textural characteristics of whipped cream. *Food Chemistry, 116*(3), 624–628. https://doi.org/10.1016/j.foodchem.2009.02.079

Zhuang, X., Gaudino, N., Clark, S., & Acevedo, N. C. (2021). Novel lecithin-based oleogels and oleogel emulsions delay lipid oxidation and extend probiotic bacteria survival. *LWT-Food Science & Technology, 136*, Article 110353. https://doi.org/10.1016/j.lwt.2020.110353

Zou, Y., Xi, Y., Pan, J., Ahmad, M. I., Zhang, A., Zhang, C., et al. (2022). Soy oil and SPI based-oleogels structuring with glycerol monolaurate by emulsion-templated approach: Preparation, characterization and potential application. *Food Chemistry, 397*, Article 133767. https://doi.org/10.1016/j.foodchem.2022.133767